phycology

MDPI

Article

Diversity of Laminar *Ulva* Species Associated with Summer "Green Tides" at Dichato Beach, Chile: An Integrative Morphological and Molecular Approach

Paula Bustos-Morales [1,2], Pilar A. Haye [2,3], María Eliana Ramírez [4], Benjamín Pinilla-Rojas [1,2], Laura Farías [2,5], Carla A. Arratia [2,3], Sergio A. Navarrete [2,6], Walter Troncoso [6] and Loretto Contreras-Porcia [1,2,*]

1 Centro de Investigación Marina Quintay (CIMARQ), Facultad de Ciencias de la Vida, Universidad Andres Bello, Santiago 8370251, Chile; p.bustosmorales1@uandresbello.edu (P.B.-M.); benjamin.pinilla.rojas11@gmail.com (B.P.-R.)
2 Instituto Milenio en Socio-Ecología Costera (SECOS), Santiago 8370251, Chile; phaye@ucn.cl (P.A.H.); laura.farias@udec.cl (L.F.); carla.arratia@alumnos.ucn.cl (C.A.A.); snavarrete@bio.puc.cl (S.A.N.)
3 Departamento de Biología Marina, Facultad de Ciencias del Mar, Universidad Católica del Norte, Coquimbo 1780000, Chile
4 Área Botánica, Museo Nacional de Historia Natural, Santiago 8500000, Chile; mramirezcasali@gmail.com
5 Departamento de Oceanografía, Facultad de Ciencias Naturales y Oceanográficas, Universidad de Concepción, Concepción 4070386, Chile
6 Estación Costera de Investigaciones Marinas, Las Cruces, Facultad de Ciencias Biológicas, Pontificia Universidad Católica de Chile, Santiago 8331150, Chile; wtroncoso10@gmail.com
* Correspondence: lorettocontreras@unab.cl or loretto.contreras@gmail.com

Abstract

Marine green tides are ecological phenomena caused by the massive proliferation of green macroalgae, particularly species of the genus *Ulva*, whose frequency and geographic extent have increased worldwide. These events are commonly associated with interacting anthropogenic and environmental drivers, including nutrient enrichment, coastal modification, climatic variability, and hydrodynamic retention. In Chile, green tides have been reported in several coastal bays, including Coliumo Bay; however, systematic studies on their species composition have been largely restricted to Algarrobo Bay, another coastal upwelling-influenced embayment located in central Chile. In this study, we investigated the laminar *Ulva* species associated with recurrent summer green tides at Dichato Beach, located in Coliumo Bay, Biobío Region, Chile. Twenty specimens were collected during the 2025 green tide and analyzed using an integrative approach that combined detailed morphological characterization with molecular analyses based on the *tuf* A and *ITS1* markers. Our results revealed the presence of three laminar, foliose, and distromatic taxa: *Ulva australis*, *Ulva stenophylloides*, and an unresolved lineage designated as *Ulva* sp. (D4). These taxa showed consistent morphological differentiation in traits such as thallus color, frond margin morphology, and perforation patterns. Phylogenetic analyses further indicated that *Ulva* sp. (D4) did not cluster with any described species included in the analyses, supporting its recognition as a distinct lineage that may represent an undescribed taxon. This study expands the known distribution of *U. australis* and *U. stenophylloides* in the southeastern Pacific and highlights the relevance of integrative taxonomy for resolving green tide diversity and supporting future ecological monitoring and management strategies in Chilean coastal systems.

Keywords: *Ulva*; green tides; macroalgal blooms; integrative taxonomy; molecular phylogeny; *tuf* A; *ITS1*; morphometry; southeastern Pacific; Chile

Check for updates

Academic Editor: Éva Ács

Received: 15 September 2026
Revised: 15 October 2026
Accepted: 18 October 2026
Published: 26 October 2026

Copyright: © 2026 by the authors. Licensee MDPI, Basel, Switzerland. This article is an open access article distributed under the terms and conditions of the Creative Commons Attribution (CC BY) license.

1. Introduction

Marine green tides are large-scale events caused by the massive proliferation of green seaweeds (Chlorophyta), resulting in high biomass accumulation along coastlines and potentially disrupting ecosystem functioning. These events are mainly associated with species of *Ulva*, *Cladophora*, and *Spirogyra*, with *Ulva* typically being the dominant genus [1–4]. This biomass reduces light penetration and consumes dissolved oxygen during respiration and decomposition processes, among other environmental impacts [3]. When stranded onshore, decomposing macroalgal biomass can produce gases such as hydrogen sulfide and methane, causing odors and potential health risks [1]. Consequently, green tides have reduced tourism and negatively affected coastal industries, including aquaculture [3–6].

Although their causes are not fully resolved, green tides are strongly linked to environmental conditions in anthropogenically altered coasts [6,7]. Main drivers include eutrophication associated with agricultural and urban nutrient inputs to coastal zones, as well as natural nutrient enrichment processes by coastal upwelling [8]. Additional factors include habitat alteration reducing competition and grazing, the expansion of artificial substrates, and rising heavy metal contamination [6,9–11]. Accordingly, *Ulva* species are effective bioindicators of marine pollution due to their rapid growth and high nutrient uptake, even at early life stages [12–14].

Large-scale green tides are recurrent worldwide. A major case occurs along the Qingdao coast (Yellow Sea, China), where summer green tides dominated by *U. prolifera* have exceeded one million tons since 2007, requiring costly removal, without even tackling the potential control of the underlying drivers [15–18]. Another hotspot of green tides is Brittany (northwestern France), where *Ulva* spp. blooms have persisted since the 1970s, loosely linked to increasing agricultural runoff since the Second World War and leading to the "Anti-Algae" plan in 2010 due to ecological and health concerns [19,20]. Together, these and many cases of smaller magnitude around the world highlight the increasing global frequency and potentially devastating extent of seaweed blooms and strandings [4,7,14].

In Chile, green tides have gained increasing attention over the past two decades due to their negative effects on local communities. Identifying the species involved and their drivers is urgently needed to prevent new introductions, support mitigation strategies, and evaluate their biotechnological potential [6]. Thus far, two major green tide systems have been recognized along the Chilean coast: the well-studied green tide in Algarrobo Bay, Valparaíso Region, and the more recently documented event at Dichato Beach, Tomé, Biobío Region, located at the proximal end of the semi-enclosed Coliumo Bay, approximately 35 km north of Concepción [6,21].

Although no formal scientific studies have yet addressed the persistent green tide at Dichato, media reports describe recurrent summer accumulations of "sea lettuce," causing strong odors, shoreline contamination, and economic losses linked to reduced tourism, suggesting dominance of laminar *Ulva* spp. [22]. There is indication that, unlike Algarrobo, green tides at Dichato are more strongly seasonal (personal observations), but such a pattern has not been clearly documented. The region, like all the Humboldt Current System, is strongly influenced by coastal upwelling. Wind-driven upwelling greatly enhances nutrient availability nearshore, fuelling primary productivity by both benthic macroalgae and phytoplankton. Riverine inputs can also be an important and still understudied source of nutrients in coastal environments [23–27]. These physical and biogeochemical processes may influence nutrient availability and environmental conditions in Coliumo Bay. However, their specific contributions to *Ulva* proliferation and green-tide accumulation at Dichato Beach remain to be determined.

Morphological identification of *Ulva* species is challenging due to their simple morphologies and high plasticity, which has led many taxa to be considered cryptic despite

clear genetic differentiation [2,28]. As of October 2026, 101 species are recognized within the genus *Ulva*, according to AlgaeBase [29]. Reliance solely on morphological characters often results in uncertain taxonomic assignments, underscoring the need for molecular approaches [4]. Consequently, DNA barcoding has become essential for species identification and phylogenetic resolution in green tides, although it remains challenging due to the ancient and highly diverse nature of green algal lineages [30]. Among the most used markers are the plastidial *tuf* A gene and the nuclear *ITS1* region, both of which provide sufficient resolution for species-level discrimination within *Ulva* [4,31–34].

Early taxonomic studies in Chile based on classical morphology reported both foliose *Ulva* spp. and tubular *Enteromorpha* spp. (now included within *Ulva*), documenting 13 tubular and 7 foliose taxa along the coast [35,36]. However, integrative morphological and molecular studies remain critically scarce. To date, *Ulva australis* has been identified using combined approaches in northern Chile (Iquique) [37], while five *Ulva* species forming annual green tides were identified in Algarrobo Bay, central Chile [4]. These comprise three laminar, distromatic species (*U. stenophylloides*, *U. uncialis*, and *U. australis*) and two tubular, monostromatic species (*U. compressa* and *U. aragoensis*). Notably, *U. stenophylloides* was documented for the first time in Chile and identified as the dominant taxon.

Additional records of *Ulva* spp. based only on morphology have been reported from Quintay (Valparaíso Region) [38], and from southern Chile, including the Cape Horn Biosphere Reserve and Magallanes [39–41]. These observations indicate diverse assemblages with laminar and tubular forms; however, morphology-based identification has proven unreliable. This taxonomic uncertainty limits species-level resolution and hinders interpretation and management of green tides. Thus, morphological, molecular and phylogenetic analyses are essential to resolve *Ulva* diversity and understand drivers of green tides formation along the Chilean coast and their potential expansion to other localities.

In this context, the present study aimed to characterize the taxonomic diversity of laminar *Ulva* specimens collected from rocky intertidal habitats surrounding Dichato Beach during a summer green-tide event, using an integrative morphological and molecular approach. By establishing the identity of the sampled taxa, this study provides baseline information for future investigations addressing the species composition, ecological dynamics, and biomass contributions of *Ulva* assemblages associated with green tides.

2. Materials and Methods

2.1. Sampling at Dichato Beach

A total of twenty individuals were collected in March 2025 at rocky shores surrounding the Dichato beach where green tides regularly occur in summer months. Dichato beach is located at the proximal (south) end of the north-facing enclosed Bay of Coliumo, Tomé (Biobío Region) in central-southern Chile (ca. 36.5° S), which protects the bay from the predominant southern waves and currents (Figure 1). Three sampling stations were located on the rocky shores to the north-east of the beach: Site D1 (36°32′12″ S, 72°56′01″ W), where six individuals were collected, is formed by an extensive quasi horizontal and highly heterogenous platform of consolidated sedimentary rock in the high intertidal zone; broken by channels, crevices and tidepools. The platform breaks into channels and granitic boulders in the mid and low shore. Site D2 (36°32′20″ S, 72°56′01″ W), where five individuals were collected, is formed by a very extensive, almost flat consolidated sedimentary rock, with shallow tidepools by few channels, no boulders, and overall lower heterogeneity than site D1. Site D3 (36°32′31″ S, 72°55′56″ W), where three individuals were collected, corresponds to mostly boulders surrounded by sand at the edge of the sandy beach. An additional sampling station was located south-west of the beach, Site D4 (36°32′47″ S, 72°56′56″ W), where six individuals were collected, corresponding to a

sedimentary platform described by Pineda [42] (1983, cited by Hödl Cruzat, 2024) as part of the Quiriquina formation of the upper Cretaceous. The platform is very extensive and flat in the mid intertidal zone, breaking into channels in the low shore. It does not extend into the upper intertidal zone, as its distribution ends abruptly at the beach, where large human-placed boulders have been installed for coastal protection.

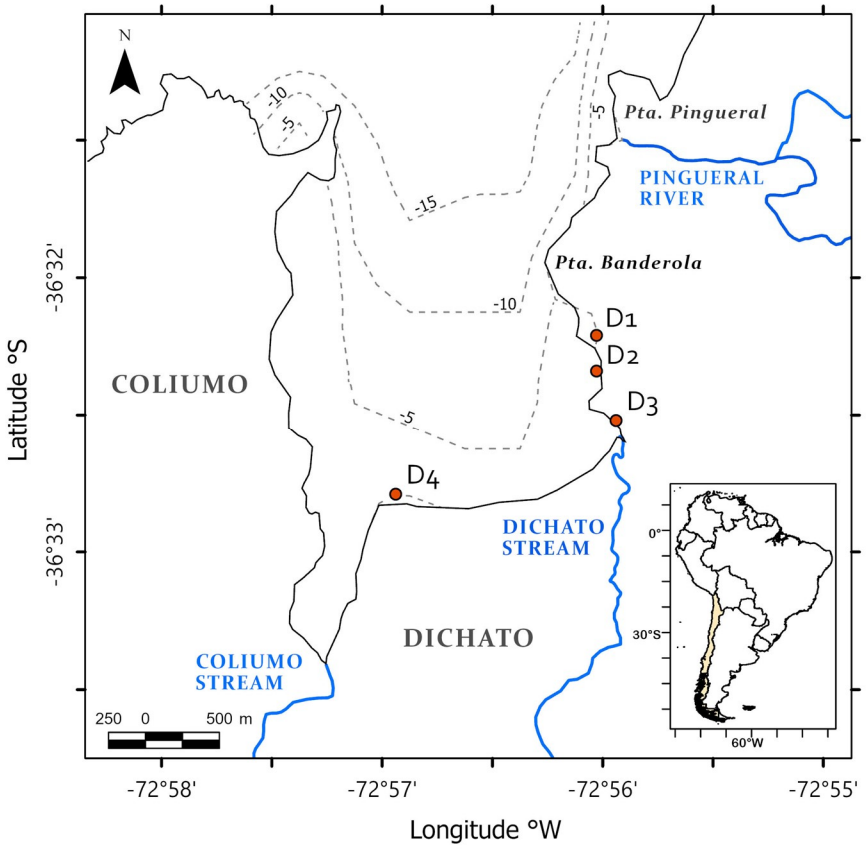


Figure 1. Location of the study area and sampling sites at Dichato Beach, Coliumo Bay, central-southern Chile. Coliumo Bay is a semi-enclosed, north-facing embayment located near Tomé, Biobío Region. Black dots indicate the four sampling sites where individuals were collected in March 2025: D1, D2, and D3 along the northeastern rocky and sandy shores around Dichato Village, and D4 on the southwestern shore. Dashed lines indicate bathymetric contours in meters and blue lines show local freshwater inputs. The inset map shows the location of the study area on the Pacific coast of South America.

Each individual was collected from the sample stations with the entire thallus intact, including the holdfast. Individuals that look different, from external attributes (thallus color, absence or presence of perforations, serrated margins of the blade, among others), were selected. Additionally, a 2 × 2 cm tissue subsample was excised from each specimen and dried in situ using silica gel desiccant (ISOLAB gel beads) with absorbent paper. Subsamples were stored individually in sterile resealable bags for subsequent molecular analyses. All specimens were then properly herborized for morphological examination and transported to the Laboratory of Ecology and Molecular Biology in Algae (LEBMA; https://www.lebma.cl/, accessed on 31 March 2025).

The specimens (Table 1) are housed in the herbarium of the National Museum of Natural History, Chile, under the numbers SGO 172447, 172449–172467 (Figure S1, Supplementary Material).

The sampling strategy was specifically designed for exploratory taxonomic characterization rather than quantitative assessment of species abundance. Attached specimens

exhibiting contrasting external morphological characteristics were purposively selected to capture morphological diversity and facilitate subsequent molecular identification. Consequently, the sampling design was not intended to provide representative estimates of taxon frequency, relative abundance, or biomass contribution. Although accumulations of green macroalgal biomass were documented at Dichato Beach during the sampling period (Figure 2), the accumulated material was not subjected to quantitative taxonomic or biomass analyses. Therefore, the taxonomic composition of the collected attached specimens should not be interpreted as directly representing the proportional species composition of the stranded green-tide biomass.

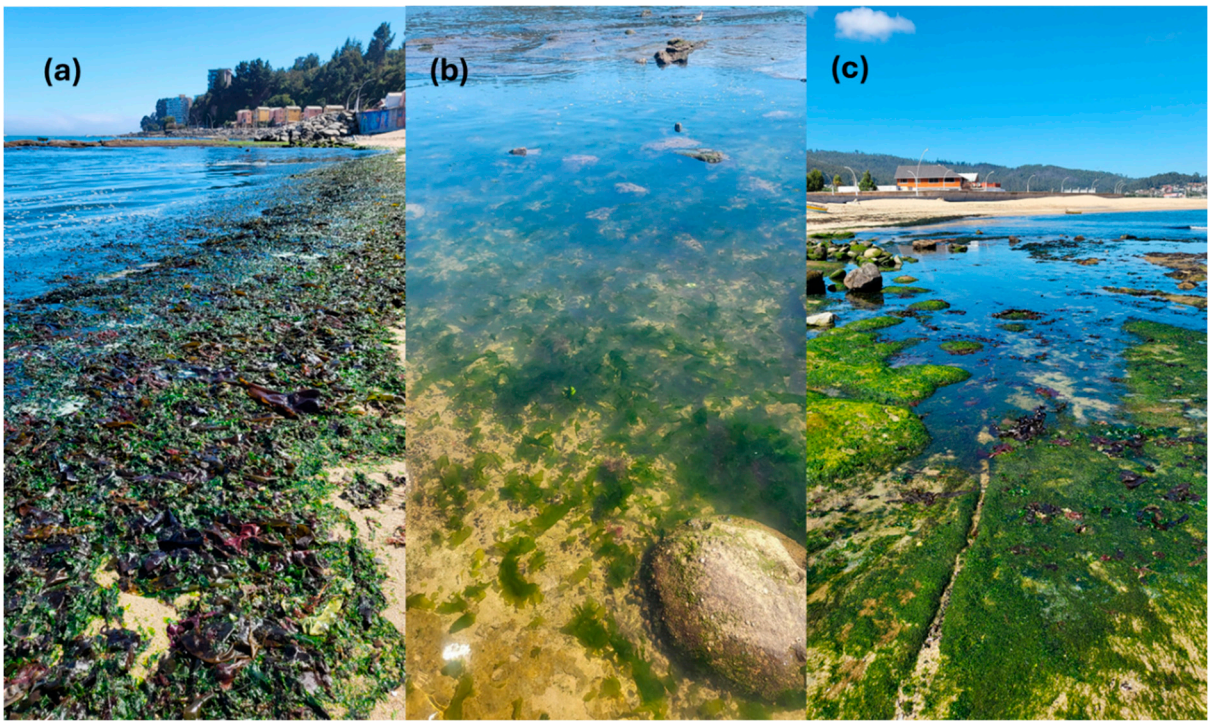


Figure 2. Photographic documentation of the green tide event at Dichato Beach (Tomé, Biobío Region, Chile), showing the spatial extent and surface accumulation of *Ulva*-dominated macroalgal biomass during the summer bloom (March 2025). (**a**) Stranded biomass on sandy substrate; (**b**) biomass in intertidal pools; (**c**) rocky intertidal zone.

Table 1. Herbarium voucher information and GenBank accession numbers for laminar *Ulva* specimens collected from the summer green tide at Dichato Beach, Chile. The table includes the taxonomic identification of each specimen, herbarium codes, SGO voucher numbers, and GenBank accession numbers for the *ITS1* and *tuf* A molecular markers. A dash indicates that no sequence was available for that marker.

Species	Herbarium Codes	SGO	Codes GenBank	
			ITS1	*tuf* A
Ulva australis	M1-D1	172447	PZ404409	PZ414580
Ulva stenophylloides	M2-D1	172449	PZ404413	PZ414584
Ulva australis	M3-D1	172450	PZ404417	PZ414587
Ulva australis	M4-D1	172451	PZ404421	PZ414591
Ulva stenophylloides	M5-D1	172452	PZ404424	PZ414594
Ulva australis	M6-D1	172453	PZ404427	PZ414597
Ulva australis	M1-D2	172454	PZ404410	PZ414581
Ulva australis	M2-D2	172455	PZ404414	PZ414585
Ulva australis	M3-D2	172456	PZ404418	PZ414588

Table 1. *Cont.*

Species	Herbarium Codes	SGO	Codes GenBank	
			ITS1	*tuf* A
Ulva stenophylloides	M4-D2	172457	PZ404422	PZ414592
Ulva stenophylloides	M5-D2	172458	PZ404425	PZ414595
Ulva australis	M1-D3	172459	PZ404411	PZ414582
Ulva australis	M2-D3	172460	PZ404415	PZ414586
Ulva australis	M3-D3	172461	PZ404419	PZ414589
Ulva sp. (D4)	M1-D4	172462	PZ404412	PZ414583
Ulva sp. (D4)	M2-D4	172463	PZ404416	-
Ulva sp. (D4)	M3-D4	172464	PZ404420	PZ414590
Ulva sp. (D4)	M4-D4	172465	PZ404423	PZ414593
Ulva sp. (D4)	M5-D4	172466	PZ404426	PZ414596
Ulva sp. (D4)	M6-D4	172467	PZ404428	PZ414598

2.2. Morphological Analysis

2.2.1. External Morphology

For external morphological analysis, the following attributes were recorded for each of the 20 herborized samples: thallus color; frond texture; margin characteristics; texture across frond zones (upper, middle, and basal); and the presence or absence of perforations. Additionally, the following morphometric variables were measured for all individuals: holdfast diameter, total thallus length, and frond width at the upper, middle, and basal zones.

2.2.2. Internal Morphology

For internal morphological analysis, a 0.5 × 0.5 cm section of herborized tissue was excised from the upper, middle, and basal regions of each of the 20 samples and rehydrated with 0.22 µm filtered seawater. Tissue sections were first examined using surface photographic records to assess cell shape and arrangement under an inverted microscope (Eclipse Ts2, Nikon, Tokyo, Japan). In addition, two transverse-section replicates per sample were prepared and documented photographically. Morphometric measurements were obtained using ImageJ (https://imagej.net/ij/), with five replicates per variable in each zone (upper, middle, and basal): cell width and height, tissue thickness, intercellular layer width, and number of cell layers. For each morphometric variable, repeated measurements within each thallus region were averaged at the individual level to avoid treating within-individual measurements as independent biological replicates. Each individual thallus was subsequently represented by a single set of morphometric values for multivariate analyses.

2.3. Phylogenetic Analyses Based on tufA and ITS1 Sequences

The 20 subsamples were preserved in silica gel desiccant (ISOLAB beads, Eschau, Germany). For each sample, a small amount of dried plant tissue was mechanically homogenized in the bead tubes supplied with the DNeasy Plan Pro Kit (Qiagen, GmbH, Hilden, Germany) using a Mini-Beadbeater-24. Genomic DNA was extracted using the DNeasy Plan Pto Kit (Qiagen), following the manufacturer's protocol.

Taxonomic identification and lineage discrimination were based on two complementary markers widely used in *Ulva* molecular taxonomy: the nuclear ribosomal *ITS1* region and the chloroplast-encoded *tuf* A gene [4]. The combined use of nuclear and plastid markers provided independent molecular evidence for species assignment and allowed comparison with reference sequences available in public databases.

For PCR amplification of the *tuf* A marker, the primers tufGF4 (5′-GGNGCNGCNCAAATGGAYGG-3′) [43] and tufAMR1 (5′-CTCGATCTCCTGGRATTACC-3′) [4] were used. The *ITS1* region was amplified using two custom-designed primers ITS F_UAM (5′-

TCTCCGTAGGTGAACCTGCG-3′), developed from a reference sequence of *Ulva australis* (accession no. OR514553.1), and ITS R_UAM (5′-GAGCWACCTACCTAGTCGG-3′), developed from a reference sequence of *Ulva rigida* (accession no. MW544059.1).

Amplifications were performed in a PCR workstation (Airclean 600, Air Science, USA, LLC, Fort Myers, FL, USA) following UV sterilization to minimize contamination. PCR reactions were carried out in a final volume of 35 µL containing 3.5 µL of template DNA, 1× PCR buffer, 0.8 mM dNTP mix, 1.3 mM $MgCl_2$, 0.6 µM of each primer, and 0.03 U/ µL of *Taq* DNA polymerase. Thermal cycling conditions included an initial denaturation at 94 °C for 10 min, 35 amplification cycles, and a final extension at 72 °C for 13 min. The annealing temperature was 47 °C for both markers. Cycling conditions for *tuf* A were 94 °C for 30 s, 47 °C for 30 s, and 72 °C for 45 s, whereas those for *ITS1* were 94 °C for 60 s, 47 °C for 60 s, and 72 °C for 120 s. PCR products were verified by agarose gel electrophoresis using 1% agarose gels prepared in 0.5× TAE buffer. Electrophoresis was performed at 90 V for 1 h, and bands were visualized under UV light. Amplified products were sequenced in both directions by Macrogen Inc. (Seoul, Republic of Korea), using the same primers employed for PCR amplification.

Forward and reverse sequences were assembled and edited to generate consensus sequences using Geneious Prime 2026.1 (www.geneious.com). All chromatograms were visually inspected, and ambiguous base calls were manually checked against peak quality. For *tuf* A, sequences were translated into amino acids to verify the open reading frame and exclude stop codons or frameshift errors. Consensus sequences were then aligned with validated GenBank reference sequences used for species identification in *Ulva*, together with sequences representing the *Ulva* lineages previously reported from Algarrobo by Mutizábal-Aros et al. [4] (2024), using the Geneious Aligner in Geneious Prime 2026.1. All newly generated sequences were deposited in GenBank under accession numbers PZ414580–PZ414598 for *tuf* A and PZ404409–PZ404428 for *ITS1* (Table 1).

Phylogenetic analyses were performed using the GTR nucleotide substitution model in the PhyML [44] and MrBayes [45] plugins in Geneious Prime. Node support was estimated with 10,000 bootstrap replicates for the maximum likelihood analyses and posterior probabilities were estimated from Bayesian analyses run for 10,000,000 iterations, with 20% of the trees discarded as *burn-in*.

2.4. Integrative Morphological and Molecular Analysis

Following morphological analyses and phylogenetic reconstruction, consistent taxonomic assignments were obtained for all 20 samples, either at the species level (*U. australis* and *U. stenophylloides*) or as an unresolved lineage (*Ulva* sp. D4). For each recovered taxon, a detailed morphological characterization was produced in accordance with the molecular and phylogenetic evidence. Additionally, exploratory Principal Component Analyses (PCA) were performed in RStudio (version 4.5.3; R Development Core Team, 2026) to assess patterns of morphological variation among the recovered *Ulva* taxa. External and internal morphological variables were analyzed separately. Individual thalli were considered the biological sampling units, and repeated morphometric measurements were summarized at the individual level before analysis. The PCA was used as an exploratory ordination approach to visualize morphological variation and overlap among taxa rather than as a formal test of species discrimination.

3. Results

Based on the integration of external and internal morphological traits with molecular data derived from DNA sequencing and phylogenetic analyses, our results reveal the presence of three taxa within the genus *Ulva*, all exhibiting laminar, distromatic thalli (Table 2). One

taxon corresponds to *Ulva australis* Areschoug, the second to *Ulva stenophylloides* L.G. Kraft, Kraft & R.F. Waller, and the third, designated as *Ulva* sp. (D4), represents an unresolved lineage that may correspond to an undescribed taxon (Figure 3, Tables 1 and 2).

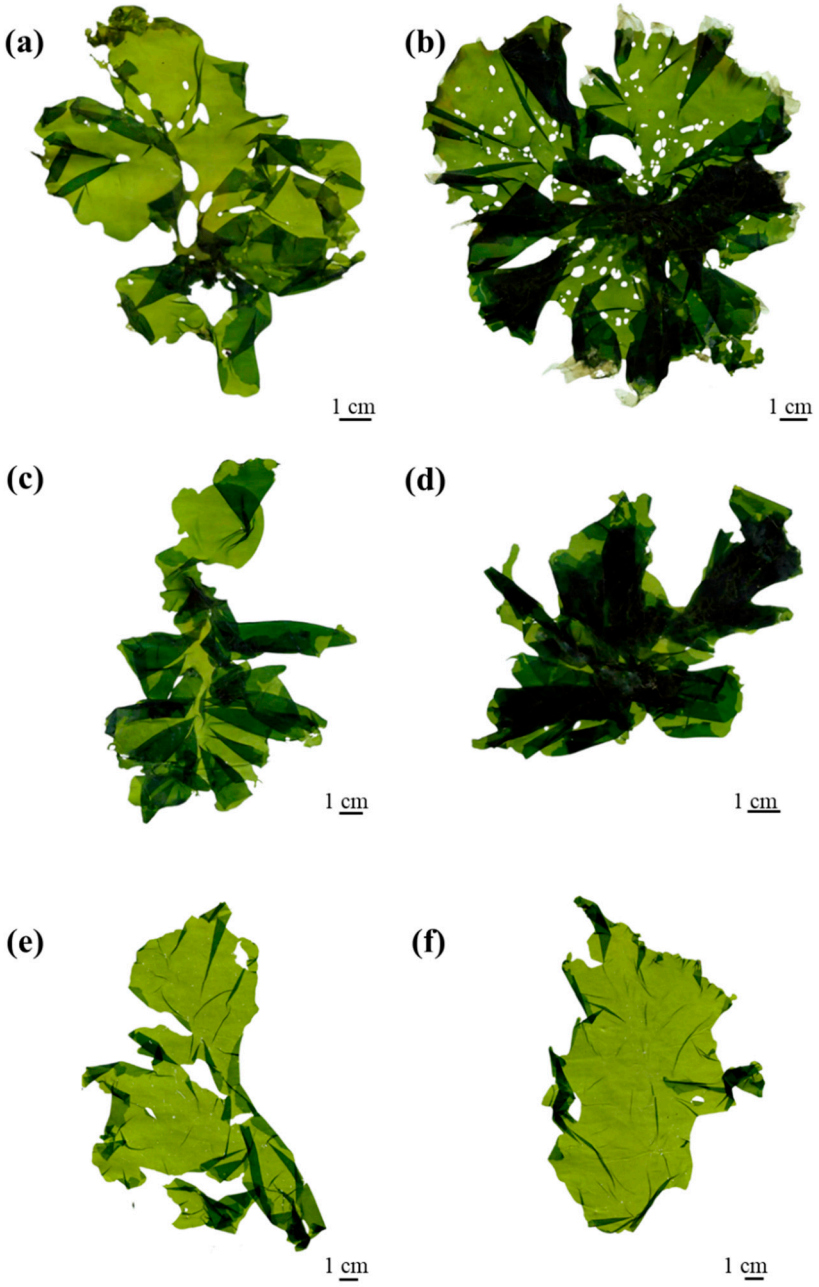


Figure 3. Thallus morphological variation among *Ulva* species associated with the green tide at Dichato, Tomé. (**a**,**b**) represent morphotypes of *Ulva australis*; (**c**,**d**) correspond to *Ulva stenophylloides*; and (**e**,**f**) depict morphotypes of *Ulva* sp. (D4).

Table 2. External morphological characteristics of the three *Ulva* taxa identified at Dichato Beach (Tomé, Chile). Diagnostic traits are highlighted in green to emphasize the main differences among taxa.

Morphological Characters	*Ulva australis*	*Ulva stenophylloides*	*Ulva* sp. (D4)
Color	Light to dark green	Light green	Very light green
Thallus form	Laminar, rosette-like	Laminar, rosette-like	Laminar, flat to expanded

Table 2. *Cont.*

Morphological Characters	*Ulva australis*	*Ulva stenophylloides*	*Ulva* sp. (D4)
Texture	Smooth	Smooth	Smooth
Upper margin	Undulate, slightly serrate	Undulate	Smooth to undulate, slightly serrate
Middle margin	Undulate	Undulate	Undulate
Basal margin	Undulate, slightly serrate	Undulate	Undulate
Holdfast shape	Round	Round	Round
Frond perforations	Present	Absent	Absent

3.1. Taxonomic Description

3.1.1. *Ulva australis*

The examined individuals exhibited a laminar thallus with variable morphotypes, including orbicular rosettes as well as lobed and foliose forms (Figure 3a,b), with coloration ranging from dark to light green. Thalli were attached to the substrate by a round holdfast measuring 4.68 ± 1.21 mm in diameter, connected to the fronds by inconspicuous stipes. Fronds were thin, smooth, and soft in texture, with few perforations. Margins were generally smooth to undulate, occasionally showing slight denticulation. On average, thalli reached 11.34 ± 11.04 cm in length, with a basal width of 0.8 ± 0.31 cm, a mid-width of 4.81 ± 1.81 cm, and an upper width of 1.05 ± 0.54 cm.

Fronds were distromatic, with a mean thickness of 55.82 ± 42.30 µm. In surface view, cells were rounded and irregularly arranged (Figure 4). In transverse section, cells were elongated, rectangular (16.26 ± 10.91 µm × 9.43 ± 3.09 µm), with rounded edges (Figure 4). The interlayer space of the frond averaged 11.94 ± 12.68 µm in thickness in the middle region. The chloroplasts occupy most of the cell volume, exhibit an irregular morphology, and contain a single pyrenoid per cell (Figure 4).

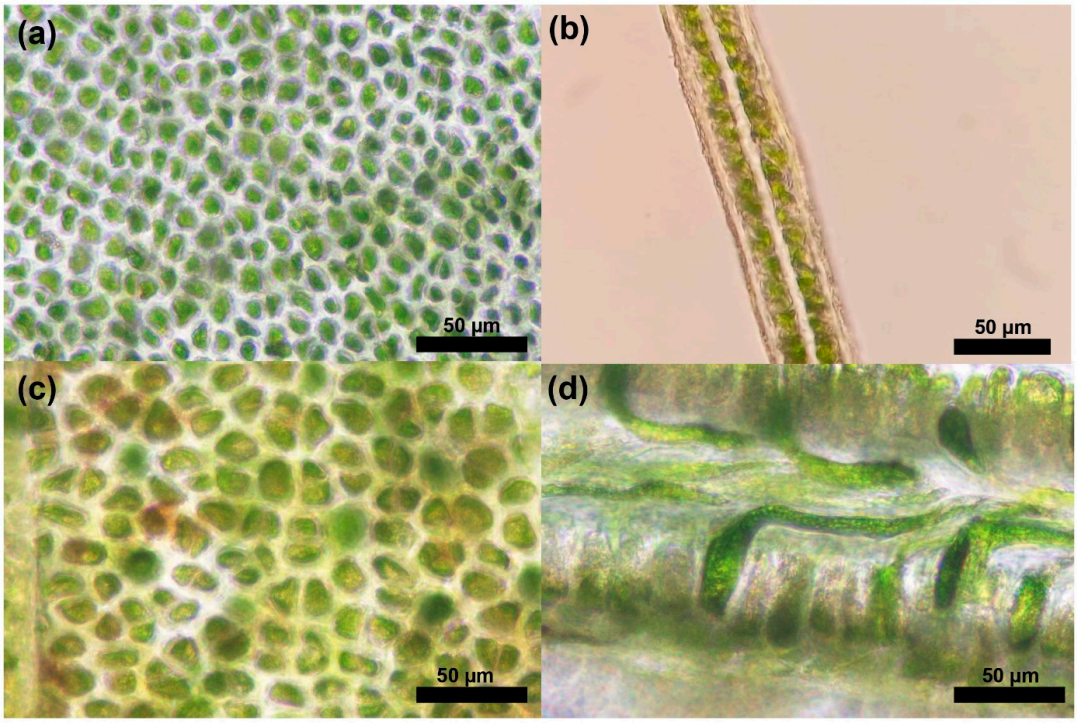


Figure 4. Tissue organization of *Ulva australis*. (**a**) Surface view of tissue from the middle thallus region; (**b**) transverse section of the middle region; (**c**) surface view of tissue from the basal region, showing a rhizoidal basal cell; and (**d**) transverse section of the basal region, where rhizoids are visible.

3.1.2. *Ulva stenophylloides*

Laminar thallus with variable morphotypes, ranging from foliose to lobed fronds of light green coloration (Figure 3c,d). Individuals were attached to the substrate by a round holdfast measuring 4.5 ± 1 mm in diameter, connected to the fronds by relatively thick stipes. Fronds were thin, smooth, and soft in texture, lacking perforations. Margins were smooth to undulate, without denticulation. On average, thalli reached 6.4 ± 0.29 cm in length, with a basal width of 0.7 ± 0.41 cm, a width at the middle region of 3.15 ± 1.81 cm, and an upper width of 1.05 ± 0.54 cm.

Fronds were distromatic, with a mean thickness of 35.55 ± 22.07 µm. In surface view, cells were subquadrate and irregularly arranged (Figure 5). In transverse section, cells were elongated and rectangular (10.76 ± 4.61 µm × 8.14 ± 3.29 µm), with rounded edges (Figure 5). The interlayer space averaged 6.64 ± 6.27 µm in thickness in the middle region. The chloroplasts occupy most of the cell volume, exhibit an oval morphology, and contain one to two pyrenoids per cell (Figure 5).

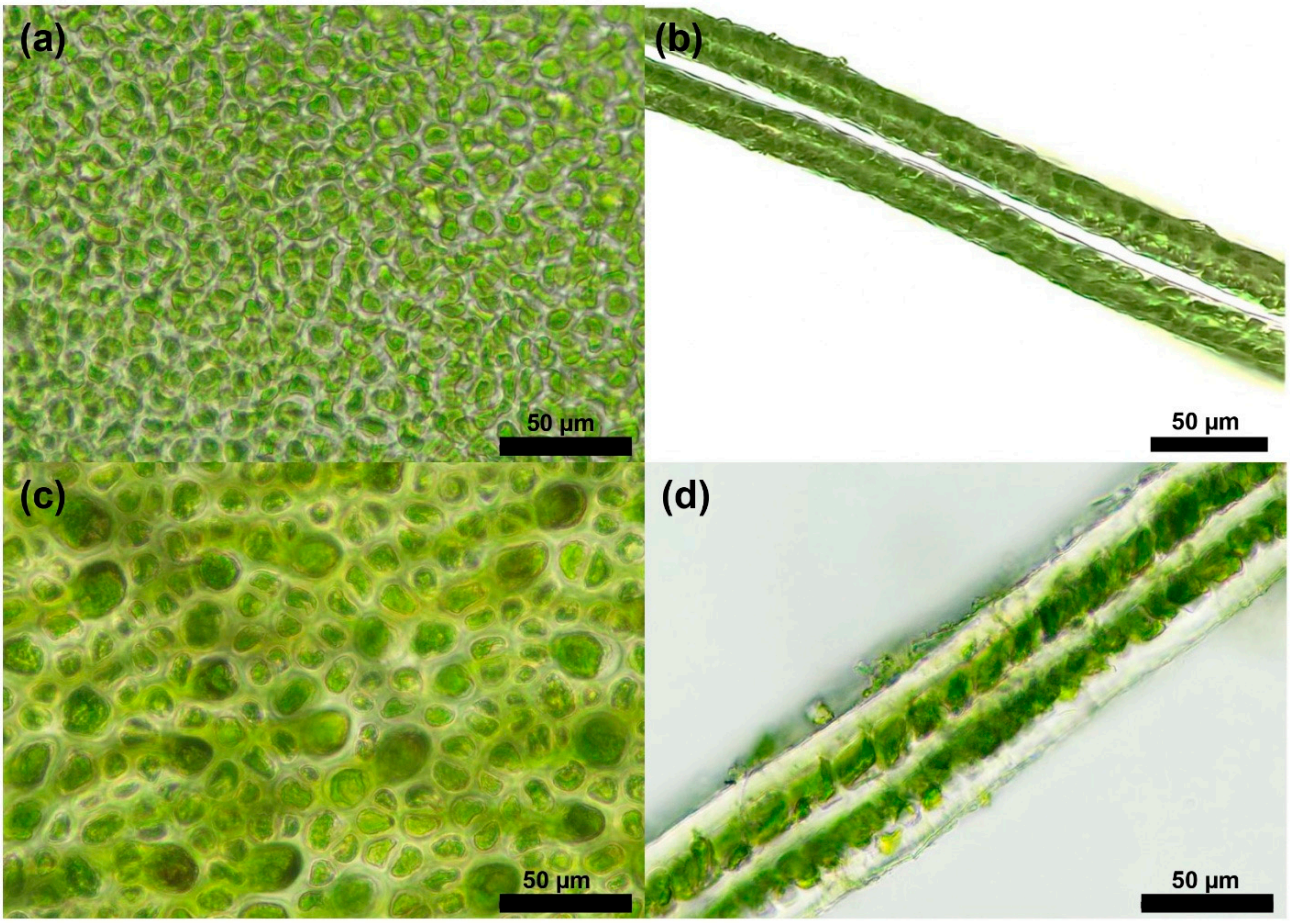


Figure 5. Tissue organization of *Ulva stenophylloides*. (**a**) Surface view of tissue from the middle thallus region; (**b**) transverse section of the middle region; (**c**) surface view of tissue from the basal region, showing a rhizoidal basal cell; and (**d**) transverse section of the basal region, where rhizoids are visible.

3.2. Ulva sp. (D4)

The examined individuals exhibited a laminar thallus with variable morphotypes. Fronds were foliose, smooth, flat, and expanded, with coloration ranging from light to very light green (Figure 3e,f). Thalli were attached to the substrate by a round holdfast measuring 1.42 ± 1.71 mm in diameter, connected to the fronds by inconspicuous stipes.

The fronds were characterized by very thin tissue, smooth, and soft in texture, lacking perforations. Margins were smooth to undulate, becoming slightly serrate in the upper region of the blade. On average, thalli reached 19.5 ± 2.35 cm in length, with a basal width of 2.02 ± 1.02 cm, a width at the middle region of 5.18 ± 2.12 cm, and an upper width of 1.1 ± 0.57 cm.

Fronds were distromatic, with a mean thickness of 22.74 ± 5.91 µm. In surface view, cells were subquadrate and irregularly arranged (Figure 6). In transverse section, cells were compact, rectangular (8.36 ± 2.53 µm × 9.19 ± 2.97 µm), with rounded edges (Figure 6). The interlayer space averaged 4.24 ± 2.02 µm in thickness in the middle region. The chloroplasts occupy most of the cell volume, exhibit an oval morphology, and contain a single pyrenoid per cell (Figure 6).

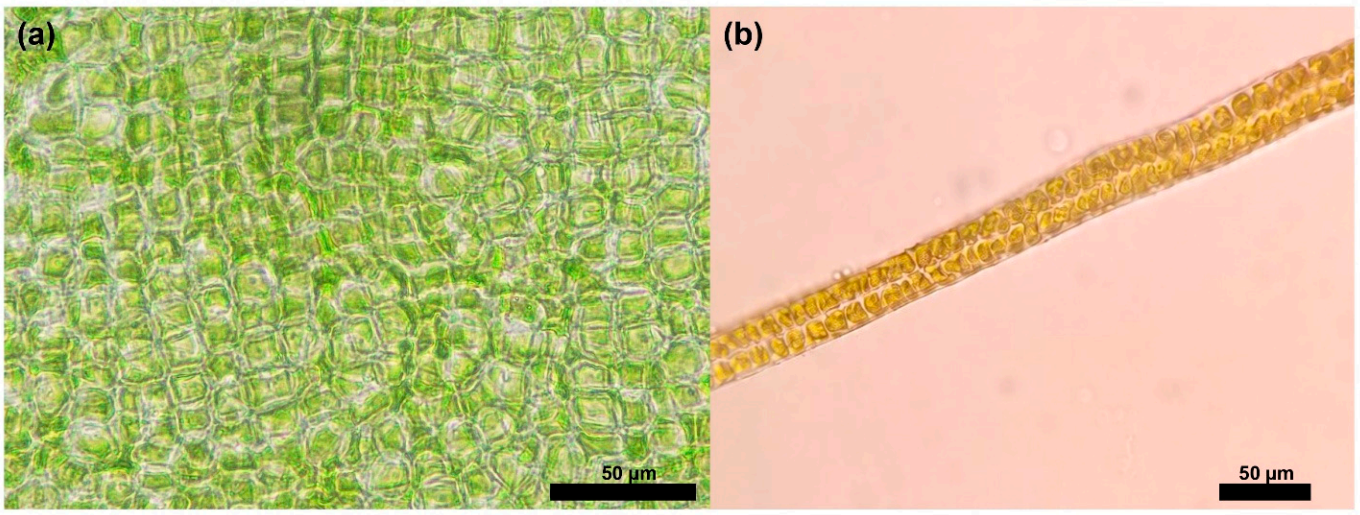


Figure 6. Tissue organization of *Ulva* sp. (D4). (**a**) Surface view of tissue from the middle thallus region; (**b**) transverse section of the middle region. Images from the basal region were not included because of their low quality, mainly resulting from the thinness of the tissue.

3.3. Molecular Phylogenetic Analyses

Phylogenetic analyses based on *ITS1* and *tuf* A sequences recovered consistent topologies and revealed the presence of three distinct *Ulva* lineages associated with green tides in Dichato (Figure 7). In both markers, specimens identified as *Ulva australis* and *Ulva stenophylloides* clustered with reference sequences retrieved from GenBank, including previously reported Chilean specimens from Algarrobo, forming well-supported clades (Figure 7).

The distinct phylogenetic placement of *Ulva* sp. (D4) in both *ITS1* and *tuf* A analyses supports its genetic differentiation from closely related taxa, particularly *U. linza* and *U. prolifera*. Maximum sequence identities of 93.96% for *ITS1* and 97.58–97.73% for *tuf* A indicate measurable divergence, although these values should not be interpreted using fixed species-delimitation thresholds, given the complex taxonomic boundaries within *Ulva*. Furthermore, the limited geographic sampling and the use of two molecular markers preclude definitive species-level delimitation. Thus, we conservatively retain the designation *Ulva* sp. (D4), pending additional molecular and taxonomic evidence.

Phylogenetic results also revealed differences in *Ulva* species composition between localities. In contrast to previous molecular analyses conducted in Algarrobo, where five *Ulva* species were detected, only three lineages were identified in Dichato (Figures 7 and 8).



Figure 7. Maximum likelihood phylograms inferred from *ITS1* and *tuf*A sequences of *Ulva* specimens associated with green tides in Dichato, Chile. Numbers at branches indicate maximum likelihood bootstrap support values (>70%) and Bayesian posterior probabilities (>0.7), respectively. Sequences generated in this study are highlighted in color, and GenBank accession numbers are indicated for reference sequences. Photographs illustrate representative morphologies of the principal lineages recovered.

99-100%
97-98.9%
94-96.9%
90-93.9%
<90%

	ITS1 \ tufA	1	2	3	4	5	6	7	8	9	10	11	12	13	14	15	16	17	18	19	20	21	22	23	24
1	M1D1		100	100	100	100	100	100	100	100	100	100	90.0		90.2	90.2	90.2	90.2	91.4	91.8	90.9	90.9	90.9	90.9	90.9
2	M1D2	99.4		100	100	100	100	100	100	100	100	100	90.0		90.2	90.2	90.2	90.2	91.4	91.8	90.9	90.9	90.9	90.9	90.9
3	M1D3	100	99.4		100	100	100	100	100	100	100	100	90.0		90.2	90.2	90.2	90.2	91.4	91.8	90.9	90.9	90.9	90.9	90.8
4	M2D2	99.4	100	99.4		100	100	100	100	100	100	100	90.0		90.2	90.2	90.2	90.2	91.4	91.8	90.9	90.9	90.9	90.9	90.8
5	M2D3	99.4	100	99.4	100		100	100	100	100	100	100	90.0		90.2	90.2	90.2	90.2	91.4	91.8	90.9	90.9	90.9	90.9	90.8
6	M3D1	98.9	98.3	98.9	98.3	98.3		100	100	100	100	100	90.0		90.2	90.2	90.2	90.2	91.4	91.8	90.9	90.9	90.9	90.9	90.8
7	M3D2	99.4	100	99.4	100	100	98.3		100	100	100	100	90.0		90.2	90.2	90.2	90.2	91.4	91.8	90.9	90.9	90.9	90.9	90.8
8	M3D3	99.4	98.9	99.4	98.9	98.9	99.4	98.9		100	100	100	90.0		90.2	90.2	90.2	90.2	91.4	91.8	90.9	90.9	90.9	90.9	90.8
9	M4D1	99.4	100	99.4	100	100	98.3	100	98.9		100	100	90.0		90.2	90.2	90.2	90.2	91.4	91.8	90.9	90.9	90.9	90.9	90.8
10	M6D1	99.4	98.9	99.4	98.9	98.9	98,3	98.9	98.9	98.9		100	90.0		90.2	90.2	90.2	90.2	91.4	91.8	90.9	90.9	90.9	90.9	90.8
11	*U. australis*	98.2	98.8	98.2	98.8	98.8	97.6	98.8	98.2	98.8	98.2		90.0		90.2	90.2	90.2	90.2	91.4	91.8	90.9	90.9	90.9	90.9	90.3
12	M1D4	87.3	87.8	87.3	87.8	87.8	87.3	88.3	87.3	87.8	87.3	87.8			99.8	99.8	99.8	99.8	97.4	97.6	94.5	94.5	94.5	94.5	94.4
13	M2D4	87.3	87.8	87.3	87.8	87.8	87.3	88.3	87.3	87.8	87.3	87.8	100												
14	M3D4	87.3	87.8	87.3	87.8	87.8	87.3	88.3	87.3	87.8	87.3	87.8	100	100		100	100	100	97.6	97.7	94.7	94.7	94.7	94.7	94.5
15	M4D4	87.3	87.8	87.3	87.8	87.8	87.3	88.3	87.3	87.8	87.3	87.8	100	100	100		100	100	97.6	97.7	94.7	94.7	94.7	94.7	94.5
16	M5D4	87.3	87.8	87.3	87.8	87.8	87.3	88.3	87.3	87.8	87.3	87.8	100	100	100	100		100	97.6	97.7	94.7	94.7	94.7	94.7	94.5
17	M6D4	87.3	87.8	87.3	87.8	87.8	87.3	88.3	87.3	87.8	87.3	87.8	100	100	100	100	100		97.6	97.7	94.7	94.7	94.7	94.7	94.5
18	*U. linza*	85.8	86.3	85.8	86.3	86.3	85.8	86.3	85.8	86.3	85.8	85.6	94.0	94.0	94.0	94.0	94.0	94.0		98.3	95.9	95.9	95.9	95.9	95.3
19	*U. prolifera*	85.8	86.3	85.8	86.3	86.3	85.8	86.3	85.8	86.3	85.8	85.6	94.0	94.0	94.0	94.0	94.0	94.0	100		95.8	95.8	95.8	95.8	95.2
20	M2D1	88.4	89.0	88.4	89.0	89.0	88.4	89.0	88.4	89.0	88.4	88.5	88.5	88.5	88.5	88.5	88.5	88.5	89.7	89.7		100	100	100	99.8
21	M4D2	88.4	89.0	88.4	89.0	89.0	88.4	89.0	88.4	89.0	88.4	88.5	88.5	88.5	88.5	88.5	88.5	88.5	89.7	89.7	100		100	100	99.8
22	M5D1	88.4	89.0	88.4	89.0	89.0	88.4	89.0	88.4	89.0	88.4	88.5	88.5	88.5	88.5	88.5	88.5	88.5	89.7	89.7	100	100		100	99.8
23	M5D2	90.8	90.8	90.8	90.8	90.8	90.8	90.8	90.8	90.8	90.8	90.3	90.2	90.2	90.2	90.2	90.2	90.2	91.5	91.5	100	100	100		99.8
24	*U. stenophylloides*	88.4	89.0	88.4	89.0	89.0	88.4	89.0	88.4	89.0	88.4	88.5	88.5	88.5	88.5	88.5	88.5	88.5	89.7	89.7	100	100	100	100	

Figure 8. Heatmap of pairwise sequence identity (%) used to evaluate molecular relationships among Dichato specimens and selected *Ulva* reference taxa, based on *ITS1* and *tuf* A markers. The lower triangle shows *ITS1* identities, whereas the upper triangle shows *tuf* A identities. Color categories indicate sequence identity ranges, as shown in the legend. Blank cells indicate comparisons for which data were not available for one of the markers.

3.4. Principal Component Analysis (PCA)

3.4.1. PCA of Sequenced Samples Based on External Morphology

The scree plot derived from the PCA of external morphological data from sequenced individuals (Figure 9a) indicates that the first two principal components explain 68.7% of the total variance (PC1 = 39.2%, PC2 = 29.5%).

The PCA biplot revealed differences in the distribution of individuals among the three recovered *Ulva* taxa, although partial overlap was evident (Figure 9a). Individuals assigned to *Ulva* sp. (D4) were predominantly distributed along positive values of PC1, associated with higher basal frond width (BFW) and frond size (FS). In contrast, *U. stenophylloides* individuals were mainly distributed toward negative values of PC2, while *U. australis* exhibited a broader distribution in ordination space, partially overlapping with *U. stenophylloides*. These patterns suggest morphological differentiation among the sampled groups, although the observed overlap indicates that external morphometric characters alone do not provide complete taxonomic discrimination.

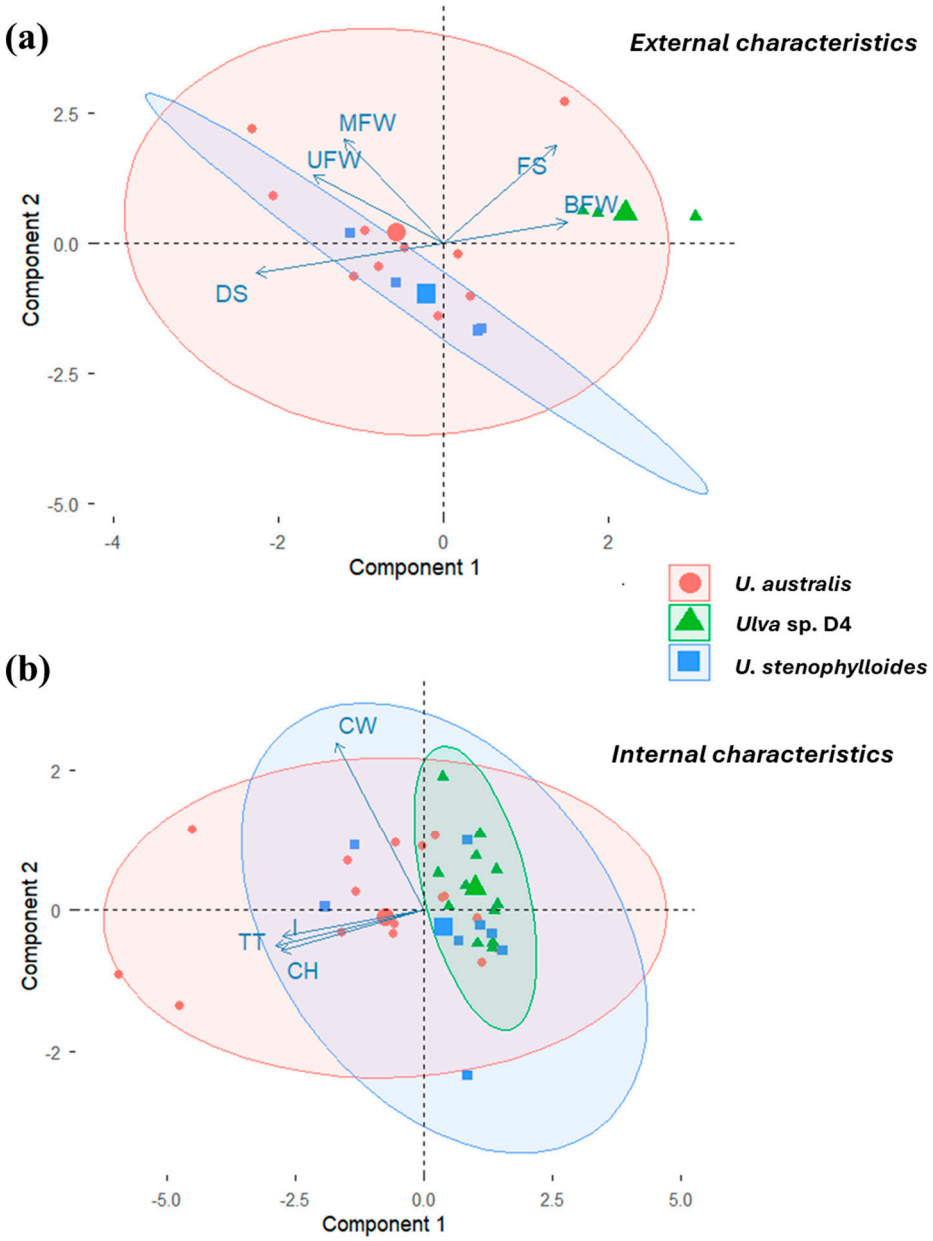


Figure 9. Principal Component Analysis (PCA) biplot based on external (**a**) and internal (**b**) morphological variables of *Ulva* spp. from Dichato Beach, showing the differentiation among the identified taxa (circles: *Ulva australis*; triangles: *Ulva* sp. (D4); squares: *Ulva stenophylloides*). BFW = basal frond width; MFW = middle frond width; UFW = upper frond width; DS = holdfast diameter; FS = frond length; CW = cell width; CH = cell height; TT = thallus thickness; and I = interlayer thickness.

3.4.2. PCA of Sequenced Samples Based on Internal Morphology

PC1 and PC2 explained 95% of the variance (76.3% and 18.7%, respectively). PC1 is primarily associated with cell height (CH) and thallus thickness (TT), whereas PC2 is mainly related to cell width (CW), showing an opposite relationship with CH and TT (Figure 9b). Individuals identified as *U. australis* were widely distributed along PC1, spanning from negative to positive values, indicating high variability in internal morphology (Figure 9b). These individuals exhibited thicker tissues (55.82 ± 42.16 µm), larger cells (16.26 ± 10.91 µm × 9.43 ± 3.09 µm), and a thicker intercellular layer (11.94 ± 12.68 µm) compared to *U. stenophylloides* and *Ulva* sp. (D4). Overall, the distribution of individuals in ordination space suggests differences in internal morphological characteristics among the sampled taxa. Nevertheless, partial overlap among groups indicates that these traits

provide complementary morphological information rather than unequivocal taxonomic discrimination. Finally, although the relatively limited sample size constrains broader inferences regarding intraspecific morphological variability, the integrative morphological and molecular evidence provides a consistent characterization of the differentiation observed among the examined lineages.

4. Discussion

The present study provides the first integrative taxonomic assessment of the laminar *Ulva* species collected from rocky intertidal habitats surrounding Dichato Beach during a summer green-tide event. Our analysis revealed the occurrence of three distinct taxa within the sampled intertidal assemblage, including *U. australis*, *U. stenophylloides*, and an unresolved lineage designated as *Ulva* sp. (D4). These findings demonstrate taxonomic heterogeneity in the local intertidal *Ulva* assemblage. Their simultaneous presence during the green-tide event does not necessarily indicate similar ecological preferences. Furthermore, because the present study focused on taxonomic characterization rather than quantitative biomass assessments, the relative contribution of each taxon to green-tide formation remains undetermined.

This finding aligns with increasing evidence that green tides worldwide are often multispecific assembles rather than being dominated by a single species, as historically assumed. The identification of *Ulva australis* and *Ulva stenophylloides* at Dichato extends their known distribution along the southeastern Pacific coast [29] and reinforces their ecological relevance in green tides-forming systems in Chile. Notably, *U. stenophylloides*, previously reported as an important component of green-tide assemblages in central Chile [4], was also present in Dichato, supporting its recognition as a persistent green tides-associated taxon in the southeastern Pacific [4,12]. Similarly, the presence of *U. australis*, a widely distributed and ecologically versatile species [29], highlights the capacity of certain *Ulva* taxa to thrive under a wide range of environmental conditions, including those influenced by anthropogenic stressors [43,46–51]. These findings emphasize the value of continued molecular surveillance of *Ulva* green tides in Chile, both to improve species delimitation and to detect possible range expansions or recurrent occurrences of introduced or cryptogenic taxa. Interestingly, *Ulva lactuca* was not detected in the Dichato assemblage, which may reflect both the geographic distance from the putative origin of the Linnaeus type material [52] (1753) and the historical misapplication of this name in morphologically based records.

The lineage herein designated as *Ulva* sp. (D4) was consistently recovered as a distinct and well-supported clade in phylogenetic analyses based on *tuf*A and *ITS1* markers. This result supports its recognition as a previously unrecognized and unresolved lineage, highlighting the still incompletely resolved diversity within the genus *Ulva*, particularly in understudied regions such as the southeastern Pacific Ocean. The occurrence of such a potentially undescribed lineage within a green tide-forming assemblage also raises important questions regarding its ecological role, physiological performance, and potential contribution to green tide persistence and intensity. Its molecular distinctiveness, together with consistent morphological traits, including very light green coloration, expanded foliose thalli with very thin fronds, absence of perforations, and reduced holdfast size, supports its recognition as a distinct lineage. However, these data alone do not justify formal species-level recognition. Although the available evidence suggests that *Ulva* sp. (D4) may represent an undescribed taxon, definitive taxonomic resolution will require additional evidence, including expanded geographic sampling, reproductive and developmental characterization, and detailed comparisons with closely related lineages. In this context, we performed a comparative morphological analysis against closely related species according

to the phylogenetic analyses, revealing no clear or consistent similarities with our specimens. For instance, *Ulva intestinalis* was originally described by Müller [53] (1778) as a smooth, hollow tube with a simple, monostromatic wall, whereas *Ulva linza* was described by Linnaeus [52] (1753) as an elongated, flattened frond lacking perforations. Therefore, we conservatively retain this taxon as *Ulva* sp. (D4), pending future taxonomic resolution.

An important limitation of the present study is that all individuals assigned to *Ulva* sp. (D4) were collected from a single sampling site (D4). Consequently, taxonomic identity and sampling location are confounded for this lineage, preventing a clear distinction between taxon-associated morphological characteristics and potential site-specific environmental influences. Given the well-documented morphological plasticity of *Ulva*, differences in thallus morphology and cellular dimensions may partly reflect local environmental conditions rather than exclusively taxonomic differentiation. Although the molecular analyses support the recognition of *Ulva* sp. (D4) as a distinct lineage, the morphometric patterns should therefore be interpreted cautiously. The multivariate analyses provided complementary information on morphological variation among the recovered *Ulva* taxa. The PCA based on external morphological traits revealed differences in the distribution of individuals, with *Ulva* sp. (D4) primarily associated with greater frond size and basal width. However, partial overlap among the sampled groups, particularly between *U. australis* and *U. stenophylloides*, indicates that external morphological traits alone are insufficient for unequivocal taxonomic discrimination. Similarly, the PCA based on internal morphological traits revealed differences in cellular dimensions and thallus thickness, although overlap among taxa was also observed. These results highlight the potential value of quantitative morphometric analyses for characterizing morphological variability within green tide assemblages, while emphasizing their limitations as independent taxonomic evidence. Accordingly, the morphological patterns identified in this study should be interpreted as complementary to, rather than definitive confirmation of, the molecular phylogenetic results.

The occurrence of multiple *Ulva* taxa in the rocky intertidal habitats surrounding Dichato Beach must be considered within the broader environmental context of Coliumo Bay. Previous oceanographic studies have described this semi-enclosed coastal system as being influenced by seasonal coastal upwelling, short-term hydrographic variability, and freshwater inputs [54–57]. The semi-enclosed morphology of the bay, its restricted exchange with adjacent shelf waters, and relatively short water residence times of approximately 2–5 d [58] make the system highly responsive to environmental forcing. During upwelling-favorable conditions, the intrusion of nutrient-rich Equatorial Subsurface Water (ESSW) promotes relatively high background nutrient concentrations, particularly during spring–summer upwelling periods. Thus, these fluctuations could be associated with nutrient inputs driven by physical processes, followed by intense biological uptake by phytoplankton [59], and possibly by macroalgae, although this was not assessed in the present study. In addition to adjacent oceanic nutrient inputs, small streams discharging into the bay may provide localized freshwater and nutrient inputs, further contributing to the environmental heterogeneity of the system [57].

Beyond seasonal variability, synoptic fluctuations associated with alternating upwelling, relaxation, and downwelling events can rapidly modify hydrographic conditions and nutrient availability within the bay [57,60]. Recent evidence from Algarrobo Bay (central Chile) shows that *Ulva stenophylloides* can sustain high growth rates under highly variable nutrient conditions [61]. High-frequency temperature records revealed short cold-water pulses, could be interpreted as nutrient-rich intrusions likely associated with internal waves [8]. Thus, temporal variability associated with upwelling, relaxation, and downwelling may enhance nutrient supply, stratification, residence time, and biomass retention [59,60], favoring multispecies *Ulva* accumulation in Coliumo Bay.

Extreme events such as marine heatwaves [62] and hypoxic episodes [63] already described in the bay may further alter the physical and biogeochemical structure of the system, potentially creating favorable windows for green tides development and persistence. Under such heterogeneous environmental conditions, coexistence of multiple *Ulva* species may be facilitated by differential physiological responses and ecological niche partitioning, allowing the persistence of complex green tide assemblages.

The multispecific assemblage of *Ulva* observed during green tide events in Coliumo Bay may also be associated with the diversity of substrates present within the system (Figure S2, Supplementary Material). The geomorphological heterogeneity of the bay, characterized by abrasion platforms, rocky shores, marine terraces, and sedimentary deposits [42], suggests the presence of different potential habitats for macroalgal settlement and growth. Although the influence of substrate characteristics on species distribution was not directly assessed in this study, such environmental heterogeneity may contribute to the coexistence of multiple *Ulva* taxa within the bay.

From an ecological and management perspective, these findings highlight the importance of resolving species composition in green tides. Different *Ulva* species may vary in growth rates, nutrient uptake efficiency, tolerance to environmental stressors, and biochemical composition [50,64–66], all of which can influence green tide dynamics and their ecological and socio-economic impacts. Moreover, accurate species identification is essential for assessing potential biotechnological applications of green tide biomass and for designing effective mitigation or valorization strategies [67,68]. Overall, this study provides a robust taxonomic baseline for understanding green tide dynamics at Dichato Beach and contributes to a growing body of evidence emphasizing the complexity and hidden diversity of *Ulva* green tides. Future research should focus on linking species identity with functional traits, environmental drivers, and green tide dynamics to better predict and manage these increasingly frequent coastal phenomena.

5. Conclusions

This study provides the first integrative taxonomic framework for the laminar *Ulva* assemblage associated with recurrent green-tides events at Dichato Beach, revealing a multispecific system that includes an unresolved, potentially undescribed lineage. By combining morphological and molecular approaches, we demonstrate that taxonomic resolution is essential to accurately characterize green tide composition and dynamics. The presence of a previously unrecognized linage highlights the still underestimated diversity of *Ulva* in the southeastern Pacific and underscores the need for continued taxonomic and phylogenetic efforts in the region.

Supplementary Materials: The following supporting information can be downloaded at: https://www.mdpi.com/article/10.3390/phycology6040114/s1, Figure S1: Herbarium voucher specimens of *Ulva* collected during this study and deposited in the Herbarium of the National Museum of Natural History, Chile (SGO), under accession numbers SGO 172447 and SGO 172449–172467. Detailed specimen information is provided in Table 1 of the main manuscript; Figure S2: Sampling station D1 corresponds to an intertidal platform composed of a low-slope rocky surface in the high intertidal and supralitoral zones, featuring a highly irregular topography characterized by crevices, channels, depressions, and numerous tidepools. This platform is sectioned into platform fragments separated by channels and boulders of variable size. The structural matrix of the platform consists of consolidated sedimentary rock, while the rounded boulders appear to be of igneous-granitic origin, generating a marked structural heterogeneity of the substrate. Panel (a) shows a view of the platform oriented towards the south, facing the inner and pro-tected section of the bay, whereas panel (b) shows the view oriented toward the north, facing the mouth or open section of the bay.

Author Contributions: P.B.-M.: Conceptualization (equal); data curation (equal); formal analysis (equal); investigation (lead); methodology (lead); software (equal); writing—original draft presentation (equal); writing—review and editing (equal). P.A.H.: Conceptualization (equal); data curation (equal); formal analysis (lead); funding acquisition (lead); investigation (equal); methodology (equal); project administration (lead); resources (lead); software (lead); supervision (equal); validation (lead); writing—original draft presentation (equal); writing—review and editing (equal). M.E.R.: Formal analysis (equal); supervision (equal); validation (equal); writing—original draft presentation (equal); writing—review and editing (equal). B.P.-R., L.F., C.A.A., W.T. and S.A.N.: Methodology (support); writing—original draft presentation (equal); writing—review and editing (equal). L.C.-P.: Conceptualization (lead); data curation (lead); formal analysis (lead); funding acquisition (lead); investigation (lead); methodology (lead); project administration (lead); resources (lead); software (lead); supervision (lead); validation (lead); writing—original draft presentation (lead); writing—review and editing (lead). All authors have read and agreed to the published version of the manuscript.

Funding: This research was supported by ANID ICM ICN2019_015, Instituto Milenio en Socio Ecología Costera (SECOS).

Data Availability Statement: All data generated or analyzed during this study are available within the published article.

Conflicts of Interest: The authors declare no conflicts of interest.

Abbreviations

tuf A	elongation factor Tu
ITS1	Internal transcribed spacer

References

1. Nelson, T.A.; Haberlin, K.; Nelson, A.V.; Ribarich, H.; Hotchkiss, R.; Van Alstyne, K.L.; Buckingham, L.; Simunds, D.J.; Fredrickson, K. Ecological and physiological controls of species composition in green macroalgal blooms. *Ecology* **2008**, *89*, 1287–1298. [CrossRef]
2. Guidone, M.; Thornber, C.; Wysor, B.; O'Kelly, C.J. Molecular and morphological diversity of Narragansett Bay (RI, USA) *Ulva* (Ulvales, Chlorophyta) populations. *J. Phycol.* **2013**, *49*, 979–995. [CrossRef]
3. Cui, B.; Liu, M.; Chen, R.; Zhang, H.; Zhang, X. Anisotropic green tide patch information extraction based on deformable convolution. *Remote Sens.* **2024**, *16*, 1162. [CrossRef]
4. Mutizabal-Aros, J.; Ramírez, M.E.; Haye, P.A.; Meynard, A.; Pinilla-Rojas, B.; Núñez, A.; Latorre-Padilla, N.; Search, F.V.; Tapia, F.J.; Saldías, G.S.; et al. Morphological and Molecular Identification of *Ulva* spp. (Ulvophyceae; Chlorophyta) from Algarrobo Bay, Chile: Understanding the Composition of Green Tides. *Plants* **2024**, *13*, 1258. [CrossRef]
5. Liu, D.; Keesing, J.K.; Xing, Q.; Shi, P. World's largest macroalgal bloom caused by expansion of seaweed aquaculture in China. *Mar. Pollut. Bull.* **2009**, *58*, 888–895. [CrossRef]
6. Navarrete, S.A.; Martínez, C.; Troncoso, W.; Tapia, F.J. *Mareas Verdes en la Bahía de Algarrobo: Conocimiento Ecológico y Oceanográfico para Informar Sobre sus Causas y Potenciales Medidas de Mitigación*; Sin Editorial: Santiago, Chile, 2024; pp. 27–67. Available online: https://biologia.uc.cl/wp-content/uploads/2025/06/MAREAS_VERDES_BAHIA_ALGARROBO.pdf (accessed on 15 October 2026).
7. Ren, C.-G.; Zhong, Z.-H.; Liu, Z.-Y.; Lin, S.; Luo, Y.-K.; Qin, S. The ever-lasting green tides: What can we do? *Heliyon* **2024**, *10*, e25220. [CrossRef]
8. Search, F.V.; Vergara, O.A.; Tapia, F.J.; Navarrete, S.A.; Figueroa, P.A.; Contreras-Porcia, L.; Saldías, G.S. Circulation and hydrographic conditions in an upwelling-influenced bay of central Chile. *J. Mar. Syst.* **2026**, *254*, 104196. [CrossRef]
9. Nelson, T.A.; Nelson, A.V.; Tjoelker, M. Seasonal and Spatial Patterns of Green Tides (Ulvoid Algal Blooms) and Related Water Quality Parameters in the Coastal Waters of Washington State, USA. *Bot. Mar.* **2003**, *46*, 263–275. [CrossRef]
10. Teichberg, M.; Fox, S.E.; Olsen, Y.S.; Valiela, I.; Martinetto, P.; Iribarne, O.; Muto, E.Y.; Petti, M.A.V.; Corbisier, T.N.; Soto-Jiménez, M.; et al. Eutrophication and macroalgal blooms in temperate and tropical coastal waters: Nutrient enrichment experiments with *Ulva* spp. *Glob. Change Biol.* **2010**, *16*, 2624–2637. [CrossRef]
11. Li, Z.; Huo, J.; Bricker, J.D. Ecological risk assessment for eutrophication and heavy metal pollution of Suyahu Reservoir sediments. *Biotechnol. Biotechnol. Equip.* **2019**, *33*, 1053–1062. [CrossRef]

12. Kraft, L.; Kraft, T.G.; Waller, F.R. Investigations into southern Australian *Ulva* (Ulvophyceae, Chlorophyta) taxonomy and molecular phylogeny indicate both cosmopolitanism and endemic criptic species. *J. Phycol.* **2010**, *46*, 1257–1277. [CrossRef]
13. Contreras-Porcia, L.; Dennett, G.; González, A.; Vergara, E.; Medina, C.; Correa, J.A.; Moenne, A. Identification of copper-induced genes in the marine alga *Ulva compressa* (Chlorophyta). *Mar. Biotechnol.* **2011**, *13*, 544–556. [CrossRef]
14. Ye, N.-H.; Zhang, X.-W.; Mao, Y.-Z.; Liang, C.-W.; Xu, D.; Zou, J.; Zhuang, Z.-M.; Wang, Q.-Y. 'Green tides' are overwhelming the coastline of our blue planet: Taking the world's largest example. *Ecol. Res.* **2011**, *26*, 477–485. [CrossRef]
15. Liu, F.; Pang, S.; Chopin, T.; Gao, S.; Shan, T.; Zhao, X.; Li, J. Understanding the recurrent large-scale green tide in the Yellow Sea: Temporal and spatial correlations between multiple geographical, aquacultural, and biological factors. *Mar. Environ. Res.* **2012**, *83*, 38–47. [CrossRef]
16. Zhang, J.; Shi, J.; Gao, S.; Huo, Y.; Cui, J.; Shen, H.; Liu, G.; He, P. Annual patterns of macroalgal blooms in the Yellow Sea during 2007–2017. *PLoS ONE* **2019**, *14*, e0210460. [CrossRef]
17. Ma, C.; Chen, H. Research on world green tide phenomenon and the green tide management at Qingdao Yellow Sea. In *OCEANS 2022 Hampton Roads*; IEEE: Hampton Roads, VA, USA, 2022; pp. 1–4. [CrossRef]
18. Tang, Y.; Wu, M.; Zhao, J.; Luan, S.; Yang, P.; Liu, L.; Liu, B.; Lv, J.; Chen, G.; Kan, H.; et al. A remote sensing framework unveiling the life-cycle dynamics and environmental drivers of *Ulva prolifera* green tides in the South Yellow Sea. *Mar. Environ. Res.* **2026**, *216*, 107920. [CrossRef]
19. Schreyers, L.; van Emmerik, T.; Biermann, L.; Le Lay, Y.-F. Spotting green tides over Brittany from space: Three decades of monitoring with Landsat imagery. *Remote Sens.* **2021**, *13*, 1408. [CrossRef]
20. Louis, J.; Ballu, S.; Rossi, N.; Lasbleiz, M.; Perrot, T.; Daniel, C.; Cellier, L.; Hénaff, F.; Richier, S. Multi-year renewal of green tides: 18 years of algal mat monitoring (2003–2020) on French coastline (Brittany region). *Mar. Pollut. Bull.* **2023**, *193*, 115173. [CrossRef]
21. Gobierno Regional del Bío Bío. *Informe Ambiental: Proceso Evaluación Ambiental Estratégica, Región del Bío Bío, Zonificación Costera Comunal Tomé*; Oficina Técnica, Comisión Regional de Uso del Borde Costero, Departamento de Planificación y Ordenamiento Territorial, División de Planificación y Desarrollo Regional del Bío Bío: Concepción, Chile, 2015. Available online: https://eae.mma.gob.cl/storage/documents/02_1er_IA_Micro_ZBC_Tome.pdf.pdf (accessed on 15 October 2026).
22. Charpentier, M. Recién en 2017 Estaría Operativa Máquina para Limpiar "Marea Verde" en Playa de Dichato. BioBioChile. Available online: https://www.biobiochile.cl/noticias/2016/01/13/recien-en-2017-estaria-operativa-maquina-para-limpiar-marea-verde-en-playa-de-dichato.shtml (accessed on 14 October 2026).
23. Escribano, R.; Castro, L.; Daneri, G.; Farías, L.; González, H.; Morales, C.; Pizarro, O.; Rosales, S. *Monitoreo de las Condiciones Bio-oceanográficas en la VIII Región, año 2004*; Informe Final FIP N°2004-20; Universidad de Concepción: Concepción, Chile, 2004. Available online: https://www.subpesca.cl/fipa/613/articles-89057_informe_final.pdf (accessed on 15 October 2026).
24. Masotti, I.; Aparicio-Rizzo, P.; Yevenes, M.A.; Garreaud, R.; Belmar, L.; Farías, L. The Influence of River Discharge on Nutrient Export and Phytoplankton Biomass Off the Central Chile Coast (33°–37° S): Seasonal Cycle and Interannual Variability. *Front. Mar. Sci.* **2018**, *5*, 423. [CrossRef]
25. Salcedo-Castro, J.; Olita, A.; Saavedra, F.; Saldías, G.S.; Cruz-Gómez, R.C.; De la Torre Martínez, C.D. Modeling the interannual variability in Maipo and Rapel river plumes off central Chile. *Ocean Sci.* **2023**, *19*, 1687–1703. [CrossRef]
26. Bustos-Espinoza, L.; Torres-Ramírez, P.; Figueroa, S.; González, P.S.; Pavez, M.A.; Jerez, R.; Saldías, G.S.; Espinoza, C.; Galán, A. Biogeochemical Response of the Water Column of Concepción Bay, Chile, to a New Regime of Atmospheric and Oceanographic Variability. *Geosciences* **2024**, *14*, 125. [CrossRef]
27. Soto-Mendoza, S.; Vergara, O.A.; Echevin, V.; Castro, L.; Cubillos, L.A.; Sobarzo, M. Biobío river freshwater discharge effect on *Engraulis ringens* early stages transport in the Gulf of Arauco (Chile) using biophysical modeling. *Estuar. Coast. Shelf Sci.* **2025**, *324*, 109438. [CrossRef]
28. Hofmann, L.C.; Nettleton, J.C.; Neefus, C.D.; Mathieson, A.C. Cryptic diversity of *Ulva* (Ulvales, Chlorophyta) in the Great Bay Estuarine System (Atlantic USA): Introduced and indigenous distromatic species. *Eur. J. Phycol.* **2010**, *45*, 230–239. [CrossRef]
29. Guiry, M.D.; Guiry, G.M. AlgaeBase. World-Wide Electronic Publication, University of Galway. Available online: https://www.algaebase.org (accessed on 15 October 2026).
30. Hall, J.D.; Fucikova, K.; Lo, C.; Lewis, L.A.; Karol, K.G. An assessment of proposed DNA barcodes in freshwater green algae. *Cryptogam. Algol.* **2010**, *31*, 529–555. Available online: https://sciencepress.mnhn.fr/sites/default/files/articles/pdf/cryptogamie-algologie2010v31f4a23.pdf (accessed on 15 October 2026).
31. Saunders, G.; Kucera, H. An evaluation of *rbcL*, *tufA*, UPA, LSU and ITS as DNA barcode markers for the marine green macroalgae. *Cryptogam. Algol.* **2010**, *31*, 487–528. Available online: https://sciencepress.mnhn.fr/sites/default/files/articles/pdf/cryptogamie-algologie2010v31f4a22.pdf (accessed on 15 October 2026).
32. Kang, J.H.; Jang, J.E.; Kim, J.H.; Byeon, S.Y.; Kim, S.; Choi, S.K.; Kang, Y.H.; Sang, R.P.; Lee, H.J. Species composition, diversity, and distribution of the genus *Ulva* along the coast of Jeju Island, Korea based on molecular phylogenetic analysis. *PLoS ONE* **2019**, *14*, e0219958. [CrossRef]

33. Kuba, G.M.; Carpio-Aguilar, B.; Eklund, J.; Freshwater, D.W. A Demonstration of DNA Barcoding-Based Identification of Blade-Form *Ulva* (Ulvophyceae, Chlorophyta) Species from Three Site in the San Juan Islands, Washington, USA. *Diversity* **2022**, *14*, 899. [CrossRef]
34. Wang, X.; Shan, T.; Sun, Y.; Li, Q.; Sun, S.; Wu, H. Molecular phylogenetic analysis and exploration of the sporulation features of *Ulva* spp. in the yellow sea of China provide insight into *Ulva prolifera* being the dominant species in green tides. *Phycol. J.* **2026**, *2*, 3. [CrossRef]
35. Ramírez, M.E.; Santelices, B. *Catálogo de las Algas Marinas Bentónicas de la Costa Temperada del Pacífico de Sudamérica*; Facultad de Ciencias Biológicas, Editorial Pontificia Universidad Católica: Santiago, Chile, 1991; pp. 28–35.
36. Hoffmann, A.; Santelices, B. *Flora Marina de Chile = Central Marine Flora of Central Chile*; Ediciones Universidad Católica de Chile: Santiago, Chile, 1997; pp. 50–70. Available online: http://bibliotecas.uchile.cl/documentos/20090528-0644c580219.gif (accessed on 15 October 2026).
37. Oróstica, M.; Calderon, M.S.; Boo, S.M.; Sandoval, C.; Edding, M. A new record of *Ulva australis* (Ulvaceae, Chlorophyta) from northern Chile. *Rev. Biol. Mar. Oceanogr.* **2017**, *52*, 621–630. [CrossRef]
38. Ramírez, M.E.; Bulboa, C.; Contreras-Porcia, L.; Mora, A.M. *Flora Marina Bentónica de Quintay*; RIL Editores: Santiago, Chile, 2018.
39. Mansilla, A.; Ávila, M.; Ramírez, M.E.; Rodríguez, J.P.; Rosenfeld, S.; Ojeda, J.; Marambio, J. Shallow Subtidial Benthic Marine Macroalgae from the Magellan Subantartic Ecorregion, Chile. *An. Inst. Patagon.* **2013**, *41*, 51–64. [CrossRef]
40. Jofre, J.; Dubrasquet, H.; Ramírez, M.A.; Navarro, N.; Macaya, E.C. *Subantartic Macroalgae Guide: Magallanes and Chilean Antartictica Region*, 1st ed.; Punta Arenas, Chile, 2021. Available online: https://www.researchgate.net/publication/356474056_Guia_de_Macroalgas_Subantarticas_Region_de_Magallanes_y_Antartica_Chilena_Subantartic_Macroalgae_Guide_Magallanes_and_Chilean_Antarctic_Region (accessed on 15 October 2026).
41. Rodríguez, J.P.; Gibelli, V.; Bahamonde, F.; Marambio, J.; Calderón, M.S.; Bustamante, D.E.; Rozzi, R.; Mansilla, A.O. First catalogue of benthic marine macroalgae from glacier-influenced environments of the Beagle Channel, deposited in the new Sub-Antarctic Cryptogamic Herbarium (SCH) of the University of Magallanes. *An. Inst. Patagon.* **2024**, *52*, 1–41. Available online: https://www.scielo.cl/pdf/ainpat/v52/0718-686X-ainpat-52-1.pdf (accessed on 15 October 2026).
42. Hödl Cruzat, E.B. *Geología y Principales Peligros Geológicos de la Península de Coliumo, Comuna de Tomé, Región del Biobío*; Memoria para optar al Título de Geólogo; Universidad de Concepción: Concepción, Chile, 2024. Available online: https://repositorio.udec.cl/bitstreams/e59740df-b412-49e8-802b-c8cdf06c8932/download (accessed on 15 October 2026).
43. Xia, Z.; Cao, X.; Li, S.; Cao, J.; Tong, Y.; Sun, Y.; Liu, J.; Zhao, S.; Cui, Q.; Zeng, Y.; et al. Distribution of *Ulva prolifera*, the dominant species in green tides along the Jiangsu Province coast in the Southern Yellow Sea, China. *J. Sea Res.* **2023**, *196*, 102436. [CrossRef]
44. Guindon, S.; Dufayard, J.F.; Lefort, V.; Anisimova, M.; Hordijk, W.; Gascuel, O. New Algorithms and Methods to Estimate Maximum-Likelihood Phylogenies: Assessing the Performance of PhyML 3.0. *Syst. Biol.* **2010**, *59*, 307–321. [CrossRef]
45. Ronquist, F.; Huelsenbeck, J.P. MrBayes 3: Bayesian phylogenetic inference under mixed models. *Bioinformatics* **2003**, *19*, 1572–1574. [CrossRef]
46. Luo, M.B.; Liu, F. Salinity-induced oxidative stress and regulation of antioxidant defense system in the marine macroalga *Ulva prolifera*. *J. Exp. Mar. Biol. Ecol.* **2011**, *409*, 223–228. [CrossRef]
47. Gupta, V.; Kushwaha, H.R. Metabolic regulatory oscillations in intertidal green seaweed *Ulva lactuca* against tidal cycles. *Sci. Rep.* **2017**, *7*, 16430. [CrossRef]
48. Bews, E.; Booher, L.; Polizzi, T.; Long, C.; Kim, J.-H.; Edwards, M.S. Effects of salinity and nutrients on metabolism and growth of *Ulva lactuca*: Implications for bioremediation of coastal watersheds. *Mar. Pollut. Bull.* **2021**, *166*, 112199. [CrossRef]
49. Vinuganesh, A.; Kumar, A.; Prakash, S.; Alotaibi, M.O.; Saleh, A.M.; Mohammed, A.E.; Beemster, G.T.S.; AbdElgawad, H. Influence of seawater acidification on biochemical composition and oxidative status of green algae *Ulva compressa*. *Sci. Total Environ.* **2021**, *806*, 150445. [CrossRef]
50. Mutizabal-Aros, J.; Meynard, A.; Contreras-Porcia, L. A Physiological Analysis of Desiccation Stress in the Green Tide Species *Ulva stenophylloides* and *Ulva uncialis* in the South Pacific. *J. Mar. Sci. Eng.* **2024**, *12*, 1893. [CrossRef]
51. Li, Y.; Yu, D.; Wang, L.; Zhao, F. Integrating Physiological and Proteomic Analysis to Unravel the Ameliorating Mechanism of Nitric Oxide on Cadmium Toxicity in *Ulva pertusa*. *Russ. J. Mar. Biol.* **2025**, *51*, 395–405. [CrossRef]
52. Linnaeus, C. *Species Plantarum, Exhibentes Plantas Rite Cognitas, ad Genera Relatas, cum Differentiis Specificis, Nominibus Trivialibus, Synonymis Selectis, Locis Natalibus, Secundum Systema Sexuale Digestas*; Impensis Laurentii Salvii: Stocklholm, Sweden, 1753.
53. Müller, O.F. *Flora Dánica*; Havniae: Copenhague, Denmark, 1778.
54. Ahumada, R. Producción y destino de la biomasa fitoplanctónica en un sistema de bahías en Chile central: Una hipótesis. *Biol. Pesq.* **1989**, *18*, 53–66. [CrossRef]
55. Sobarzo, M.; Bravo, L.; Donoso, D.; Garcés-Vargas, J.; Schneider, W. Coastal upwelling and seasonal cycles that influence the water column over the continental shelf off central Chile. *Prog. Oceanogr.* **2007**, *75*, 363–382. [CrossRef]

56. Silva, N.; Rojas, N.; Fedele, A. Water masses in the Humboldt Current System: Properties, distribution, and the nitrate deficit as a chemical water mass tracer for Equatorial Subsurface Water off Chile. *Deep-Sea Res. II Top. Stud. Oceanogr.* **2009**, *56*, 1004–1020. [CrossRef]
57. Tenorio, S.E.; Narváez, D.; Soto-Mardones, L.; Farías, L. Short-term variability of dissolved methane in surface waters of an upwelling bay off central Chile. *Environ. Res. Commun.* **2026**, *8*, 041012. [CrossRef]
58. Sobarzo, M. *Patrón General de Circulación (en Condiciones Invernales) de Bahía Coliumo (36°32′ S; 72°56′ W), Concepción, Chile*; Informe de unidad de investigación para optar al título de Biólogo Marino; Universidad de Concepción: Concepción, Chile, 1984.
59. Daneri, G.; Lizárraga, L.; Montero, P.; González, H.E.; Tapia, F.J. Wind forcing and short-term variability of phytoplankton and heterotrophic bacterioplankton in the coastal zone of the Concepción upwelling system (Central Chile). *Prog. Oceanogr.* **2012**, *92–95*, 92–96. [CrossRef]
60. Aguirre, C.; Garreaud, R.; Belmar, L.; Farías, L.; Ramajo, L.; Barrera, F. High-frequency variability of the surface ocean properties off central Chile during the upwelling season. *Front. Mar. Sci.* **2021**, *8*, 702051. [CrossRef]
61. Navarrete, S.A.; González, A.E.; Faúndez, J.; Contreras-Porcia, L.; Núñez, A.; Rivas, J.; Chacano, S.; Farías, L.; Saldías, G.S.; Tapia, F.J. Growth rates and response to nutrient variability in the green tide forming alga *Ulva stenophylloides* from Algarrobo Bay, Chile. *Mar. Environ. Res.* **2025**, *210*, 107338. [CrossRef]
62. Valdés-Castro, V.; Narváez, D.; Farías, L.; Quiñones, R.; Fernández, C.; Molina, V. Thermal extremes events in a coastal upwelling system: Biogeochemical signals from marine heatwaves, cold spells, and transient warming event. *Sci. Rep.* **2026**, *16*, 12351. [CrossRef]
63. Hernández-Miranda, E.; Veas, R.; Anabalón, V.; Quiñones, R.A. Short-term alteration of biotic and abiotic components of the pelagic system in a shallow bay produced by a strong natural hypoxia event. *PLoS ONE* **2017**, *12*, e0179023. [CrossRef]
64. Jiang, H.-P.; Gao, B.-B.; Li, W.-H.; Zhu, M.; Zheng, C.-F.; Zheng, Q.-S.; Wang, C.-H. Physiological and Biochemical Responses of *Ulva prolifera* and *Ulva linza* to Cadmium Stress. *Sci. World J.* **2013**, *2013*, 289537. [CrossRef]
65. Lubsch, A.; Timmermans, K. Uptake kinetics and storage capacity of dissolved inorganic phosphorus and corresponding N:P dynamics in *Ulva lactuca* (Chlorophyta). *J. Phycol.* **2018**, *54*, 215–223. [CrossRef]
66. Miao, X.; Zhu, X.; Ma, X.; Xia, L.; Xiao, J.; Fan, S.; Zhang, X.; Wang, Z.; Zang, Y. Morphological plasticity and physiological adaptations of *Ulva prolifera* along the drifting path of green tides in the Yellow Sea. *Mar. Pollut. Bull.* **2026**, *224*, 119067. [CrossRef]
67. Toro-Mellado, F.; Piña, F.; Baltrusch, K.L.; Inoubli, S.; Flórez-Fernández, N.; Torres, M.D.; Contreras-Porcia, L.; Domínguez, H. Potential applications of *Ulva* spp. *Food Biosci.* **2025**, *71*, 107256. [CrossRef]
68. Wichard, T.; Mapelli-Brahm, P.; Barba, F.J.; Domingues, R.; Guttman, L.; Hutarova, L.; Loureiro, J.A.; Unal, D.; Koseoglu-Yilmaz, P.; Zammit, G.; et al. Green seaweed *Ulva* spp. bioprocessing: Bioactive molecules, emerging extraction technologies, and industrial applications in the circular bioeconomy. *Bioresour. Technol.* **2026**, *445*, 134066. [CrossRef]

Disclaimer/Publisher's Note: The statements, opinions and data contained in all publications are solely those of the individual author(s) and contributor(s) and not of MDPI and/or the editor(s). MDPI and/or the editor(s) disclaim responsibility for any injury to people or property resulting from any ideas, methods, instructions or products referred to in the content.